Bioresource Technology 116 (2012) 403–412

Contents lists available at SciVerse ScienceDirect

Bioresource Technology

journal homepage: www.elsevier.com/locate/biortech

Gasification of pelletized biomass in a pilot scale downdraft gasifier

Marco Simone *, Federica Barontini, Cristiano Nicolella, Leonardo Tognotti

Università di Pisa, Dipartimento di Ingegneria Chimica, Chimica Industriale e Scienza dei Materiali, Largo Lucio Lazzarino, 2 56126 Pisa, Italy
Centro di Ricerca Interuniversitario Biomasse da Energia, Via vecchia di Marina, 6, 56122 Pisa, Italy

ARTICLE INFO

Article history:
Received 27 January 2012
Received in revised form 27 March 2012
Accepted 29 March 2012
Available online 6 April 2012

Keywords:
Gasification
Biomass pellets
Pilot plant
Syngas
Pressure drop

ABSTRACT

This work presents a pilot-scale investigation aimed at assessing the feasibility and reliability of biomass pellet gasification. Wood sawdust and sunflower seeds pellets were tested in a 200 kW downdraft gasifier operating with air as gasifying agent. The gasification of pelletized biomass led to rather high and unstable pressure drops, reducing the gasifier productivity and stability. Furthermore the generation of fine residues compromised the operation of wet ash removal systems. On the other hand, good syngas compositions (H_2 17.2%, N_2 46.0%, CH_4 2.5%, CO 21.2%, CO_2 12.6%, and C_2H_4 0.4%), specific gas production (2.2–2.4 N m^3 kg^{-1}) and cold gas efficiency (67.7–70.0%) were achieved. For these reasons pelletized biomass should be considered only as complementary fuel in co-gasification with other feedstock.

1. Introduction

Biomass gasification allows the production of several products with different end use as fuels or intermediates for chemical synthesis. Biomass gasification with air in downdraft gasifiers coupled to an IC-engine is one of the most common small scale applications due to the low tar content of the syngas and the high fuel conversion (Martinez et al., 2012). However, tight feedstock specifications such as low moisture and narrow size distribution (Martinez et al., 2012; Simone et al., 2009) limit the reliability and diffusion of this technology. Most studies on downdraft gasifiers involve woody materials as feedstock, cut in different shapes such as chips or briquettes. Sharan et al. (1997) characterized a gasification plant by using several types of wood as feedstock, demonstrating the feasibility of power production by means of an internal-combustion engine. On the other hand, some issues related to the wastewater disposal were pointed out (Hassler et al., 1997). Zainal et al. (2002) performed a series of experiments in a complete gasifier-IC engine plant and reported the performance of the system for different air–fuel ratios and different woody fuels with cubic shape. Sharma (2011) performed tests with an open-top downdraft gasifier using Acacia briquettes as feedstock; much attention was paid to the gasifier behaviour in terms of pressure drops and gas flowrate. As pointed out by Erlich and Fransson (2011), it is crucial to expand the range of fuels which can be fed to gasifiers, to overcome supply limitations related to the seasonality of specific biomass feedstock. Besides wood feedstocks, hazelnut shells also prove to be suitable for downdraft gasification (Dogru et al., 2002; Midilli et al., 2001). However other agro-industrial residues do not exhibit the same mechanical properties of chipped wood or nuts. For instance, Wander et al. (2004) reported operational problems in the gasification of wood sawdust due to the bed mechanic characteristics. Consequently these residues need to be conditioned before being processed in downdraft gasifiers. Pelletization is a suitable option for biomass conditioning, allowing production of stable dry fuels of uniform size from different biomass residues. Erlich and Fransson (2011) carried out a detailed work to assess the gasification of pelletized agricultural residues, not suitable for gasification as raw material (e.g. bagasse). These authors take into account the effect of equivalence ratio and they analyze the evolution of the pelletized material and its influence on the gas pressure drop across the char bed. Some of the aforementioned works were carried out on small scale reactors (throughput from 1 to 5 kg h^{-1}) (Dogru et al., 2002; Erlich and Fransson, 2011; Sheth and Babu, 2010). However, the demonstration of technological reliability for downdraft gasification should rely on pilot scale tests (Garcia-Bacaicoa et al., 2008; Pathak et al., 2008; Sharan et al., 1997).

In this work gasification tests of two pelletized biomass in a pilot scale downdraft gasifier with a thermal throughput of 200 kW were carried out. The study aims at:

- assessing the feasibility and reliability of the gasification process when dealing with pelletized biomass and residues;
- providing new process data for a complete evaluation of the performance of a downdraft gasifier.

* Corresponding author. Tel.: +39 0502217850; fax: +39 0502217866.
E-mail address: marco.simone@diccism.unipi.it (M. Simone).

0960-8524/$ - see front matter © 2012 Elsevier Ltd. All rights reserved.
http://dx.doi.org/10.1016/j.biortech.2012.03.119

List of notations

CGE	cold gas efficiency, –
ER	equivalence ratio, –
LHV	lower heating value, (solid) MJ kg^{-1} (gas) MJ Nm^{-3}
P_j	pressure in the annular jacket of the gasifier, mmH_2O
P_n	pressure at the nozzle outlet inside the gasifier, mmH_2O
P_0	atmospheric pressure, mmH_2O
PS	specific gas production, Nm^3 kg^{-1}
X	pressure ratio, $X = \Delta P_n/\Delta P_j$
ΔP_g	pressure drop across the gasifier bed, mmH_2O
ΔP_j	pressure difference between the atmospheric pressure and the pressure in the annular jacket of the gasifier, mmH_2O
ΔP_n	pressure difference between the atmospheric pressure and the pressure at the nozzle outlet inside the gasifier, mmH_2O

2. Experimental

2.1. Biomass feedstock

Two pelletized materials were used as feedstock: wood sawdust pellet (hereafter named WSP) supplied by a local producer and pelletized meal produced from sunflower seeds pressing (hereafter named SMP) as described in Barontini et al. (2011). While WSP complies with the specifications required by the gasifier vendor (CAEMA Engineering, Cremona, Italy) for the use in the gasifier (as reported in Barontini et al., 2011), ash and nitrogen contents in SMP are too high. This may cause clinker formation at the bottom grid of the downdraft gasifier and lead to high generation of nitrogen compounds (for instance NH_3) in the syngas. To avoid these problems, a mixture of 50%WSP–50%SMP on a weight basis (hereafter named MIX) was produced to evaluate the use of SMP in the downdraft gasifier. The properties of the two materials are reported in Table 1. The properties of MIX were achieved by analyzing several samples of milled mixture. The resulting MIX is closer to the vendor specifications than SMP itself; however the ash and nitrogen contents are still slightly beyond the limits. Because of the high lower heating value (LHV), pelletized materials are well suited as fuels. In particular, SMP exhibits a high energy content, which makes it an attractive fuel. The size distribution of WSP and SMP is very homogeneous. WSP and SMP have both cylindrical shape, with a diameter of 6 mm and 10 mm, respectively. The length range is 10–30 mm for WSP and 30–60 mm for SMP. Pelletized biomass fuels have high particle and bulk densities compared to other biomass.

2.2. Pilot scale gasification facility

Fig. 1a shows the flow-sheet of the gasification facility. The plant is designed to operate with woodchips. The biomass is fed to the top of the gasifier via a screw conveyor. The plant is operated slightly below atmospheric conditions due to a fan-blower positioned at the end of the gas clean-up line, which drives air to enter the gasifier through four nozzles positioned in the throated section of the gasifier. The gas flow-rate can be controlled by means of a valve positioned on the by-pass of the blower. The biomass is supported on a grate at the bottom of the gasifier. As the gasification reactions occur, the biomass size shrinks down, and the residue (vegetal charcoal) falls under the grate. The charcoal is washed away from the bottom plate by water flow to a settling tank and recovered with a screw conveyor. The produced syngas moves upward from the bottom of the gasifier in an external ring and enters the clean-up system. The clean-up system consists of a cyclone, a venturi scrubber, a chiller-condenser, two sawdust filters and a bag filter which are designed to remove tar, particulates and water from the syngas and make it suitable for combustion in an internal-combustion engine. In this set-up configuration, after cleaning the syngas is burned in a flare.

The gasification plant operation is based on a water handling system. Exhaust water is produced both from charcoal removal and gas cleaning. This is delivered to a first tank (collection tank) where part of the solid residues are removed, and then to the equalization tank where water is further clarified by settling and cooled in a cooling tower.

The nominal thermal input of the gasifier is 200 kW as reported in Simone et al. (2011a). A section of the downdraft gasifier is showed in Fig. 1b. The upper section of the gasifier is a reverse cone (height 1.6 m, upper diameter 0.55 m, lower diameter 1 m) fitted on a lower cylindrical body (diameter 1 m, height 1 m). The throated section (upper diameter 1 m, lower diameter 0.3 m) is positioned in the cylindrical body. Four nozzles distribute air in the middle of the throated section forming the oxidation zone where combustion reactions occur. The section above is called drying and devolatilization zone. The section below the throat is called reduction zone.

Table 1
Properties of the pelletized biomass and solid samples (ar: as received, daf: dry, ash free).

	Units	WSP	MIX	C1	C3	C5	BED	PO	PC
Moisture ar	%	9.5	12	–	–	–	–	–	–
VM dry	%	80.63	76.54	7.79	7.65	5.96	55.35	27.85	19.63
FC dry	%	17.27	18.47	87.63	83.70	86.14	41.42	24.66	60.53
ASH dry	%	2.10	4.99	4.58	8.65	7.90	3.23	47.49	19.84
C daf	%	48.91	50.51	81.63	84.79	84.60	62.24	n.d.	68.41
H daf	%	5.80	6.22	1.28	0.44	0.20	4.51	n.d.	1.30
N daf	%	0.18	1.98	0.78	0.64	0.65	1.31	n.d.	0.90
O daf	%	by diff.	by diff.	by diff.	by diff.	by diff.	by diff.	n.d.	by diff.
LHV dry	MJ kg^{-1}	18.43	19.54	25.89	25.11	24.97	–	–	–
Length	mm	10–30	10–60	10	1–2	1–2	–	–	–
Diameter	mm	6	6–10	10	1–2	1–2	–	–	–
Particle density	kg m^{-3}	1120	1105	–	–	–	–	–	–
Bulk density	kg m^{-3}	650	641	–	–	–	–	–	–

n.d.: not determined.

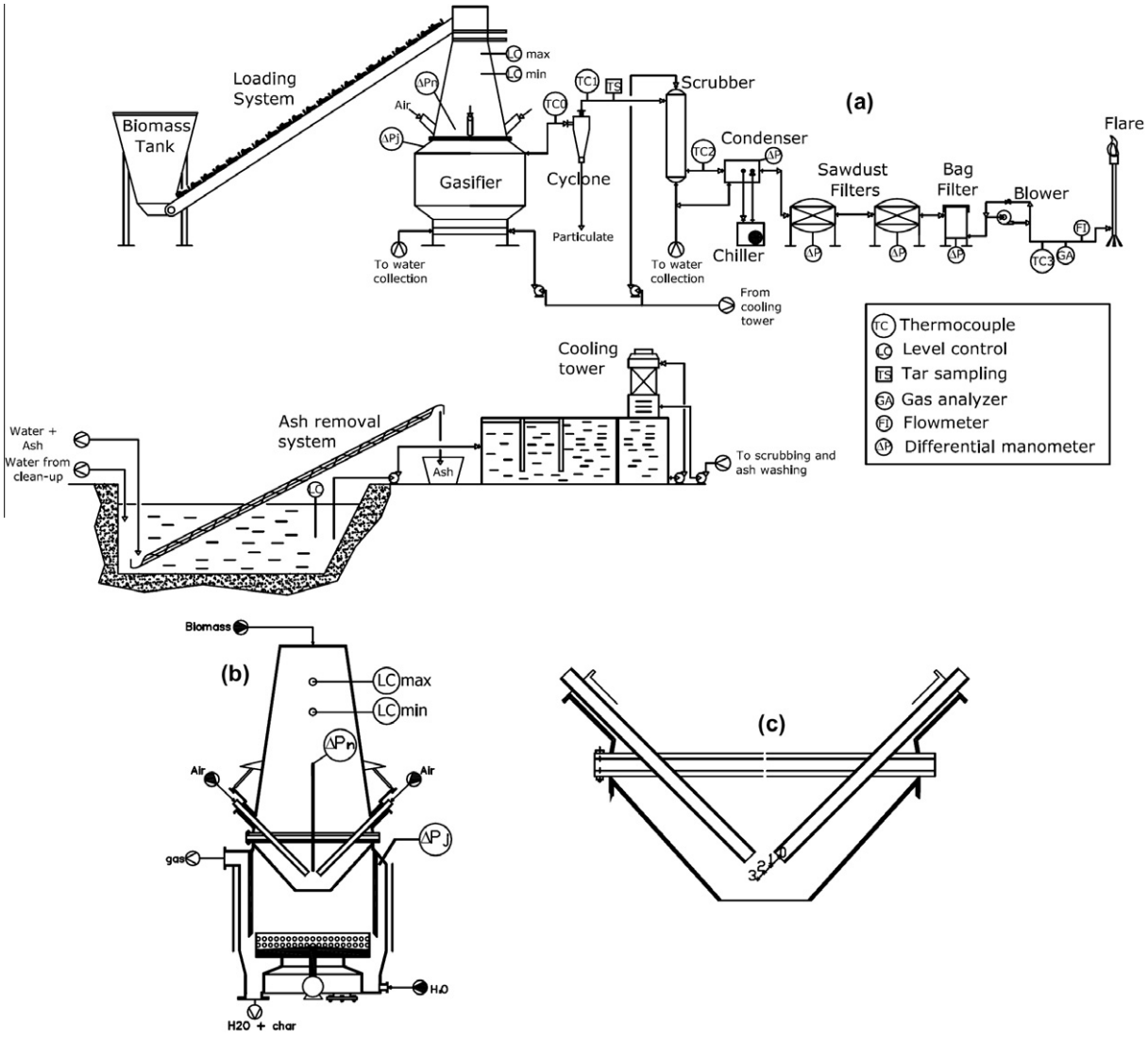

Fig. 1. (a) Flow-sheet of the gasification plant, (b) section of the gasifier, (c) position of the thermocouple inside the gasifier.

2.3. Process variable monitoring

The plant is equipped with measuring devices in order to monitor the process variables. Four J-thermocouples have been installed along the clean-up line (see Fig. 1a): TC0 – gasifier outlet; TC1 – cyclone outlet; TC2 – scrubber outlet; TC3 – blower outlet. These allow to continuously monitor the gas temperatures in the four positions. K-thermocouples connected to a portable datalogger are used to evaluate the temperature into the gasifier through the gasifier nozzles.

Differential manometers are available in the plant and provide the following data (see Fig. 1b):

- ΔP_j is the pressure difference between the atmospheric pressure (P_0) and the pressure in the annular jacket of the gasifier (P_j):

$$\Delta P_j = P_0 - P_j \tag{1}$$

- ΔP_n is the pressure difference between the atmospheric pressure (P_0) and the pressure at the nozzle outlet inside the gasifier (P_n):

$$\Delta P_n = P_0 - P_n \tag{2}$$

The pressure drop across (ΔP_g) the gasifier bed can be evaluated as the difference between ΔP_j and ΔP_n:

$$\Delta P_g = \Delta P_j - \Delta P_n \tag{3}$$

The syngas flow-rate is measured by means of a flow-meter positioned after the blower.

2.4. Plant control and management

The gasification plant is partially automated by means of a programmable logic controller (PLC). To start-up the gasification process, the gasifier is ignited using a propane flare inserted in each nozzle. As the blower drives air through the nozzles the flames can reach the throat of the gasifier and start the biomass combustion.

The control of the gasifier operation requires two procedures:

(1) Regulating the discharge frequency of the gasifier bottom grid.
(2) Modulating the syngas flow-rate by means of the by-pass valve of the blower.

The operating parameter used to monitor the gasifier behaviour is the ratio between the readings of the differential manometer ΔP_n and ΔP_j (see Eqs. (1) and (2))

$$X = \frac{\Delta P_n}{\Delta P_j} \quad (4)$$

For high values of X (i.e. when ΔP_n approaches ΔP_j), the pressure drop across the bed is negligible. This may be due to by-pass of the bed through preferential channels as well as to the decrease of the bed depth, with the gasifier switching to combustion regime due to the reduced availability of biomass. For low values of X (typically when ΔP_n gets below 5% of the ΔP_j), thickening of the bed or loss of permeability is taking place. Both conditions should be avoided because this may lead to poor syngas quality, high tar content and low biomass conversion. The optimal interval of X is 0.050–0.200.

The ratio X can be controlled by regulating the frequency discharge from the bottom grid, choosing among five frequencies. As the pressure drop across the bed increases, the discharge ratio has to be increased in order to avoid bed thickening. On the other hand, if the pressure drop starts to reduce, the frequency has to be reduced to allow for bed build up.

Another operating parameter which can be controlled is the opening of the by-pass valve positioned before the blower (see Fig. 1a). The start up and warming up of the plant are carried out with open by-pass, so to keep the plant at its minimal capacity. As the pressure becomes stable it is possible to progressively close the by-pass valve to increase the air feeding to the plant and thus the syngas flow-rate. This usually destabilizes the pressure drop across the bed. In these cases the discharge frequency has to be adjusted to recover stable conditions.

The biomass content of the gasifier is kept constant by means of a level control at the top of the gasifier.

2.5. Sampling

The gasification plant is equipped with two systems for gas sampling and analysis which are positioned at the blower outlet: a micro gas chromatograph (GC) and a Fourier Transformed Infra-Red Spectrometer (FTIR). The first one was used during the testing so it is described in the following. Liquids and condensate were sampled with an in house developed device (described in Simone et al., 2011b) connected at the cyclone outlet (Fig. 1a).

After the experimental tests it was possible to collect solid samples from the gasifier bed as well as particles from the cyclone discharge tank and bottom residues from the collection tank.

2.6. Analytical instruments and procedures

The characterization of biomass feedstock as well as of the different product fractions sampled during gasification tests (solid, liquid and gas samples) was carried out following the methodologies briefly described herein.

A standard procedure for solid characterization (biomass feedstock and solid samples collected in gasification tests) was developed, including Proximate Analysis (Moisture, Volatile Matter, Fixed Carbon and Ash content), Ultimate Analysis (Carbon, Hydrogen and Nitrogen content) and Heating Value.

The moisture content was evaluated as the weight loss of the sample after drying in a ventilated oven at 105 °C for 12 h. All analyses, but moisture determination, were carried out on milled and dried samples. Volatile Matter (VM), Fixed Carbon (FC) and Ash content were determined by thermogravimetric (TG) analysis. A TA Q-500 thermobalance was employed for TG analysis. Ultimate analysis was carried out with a LECO TruSpec CHN Elemental Determinator. A LECO AC-500 Isoperibol Calorimeter was used for Higher Heating Value (HHV) determination. Lower Heating Value (LHV) was calculated on the basis of HHV and sample hydrogen content.

Gas Chromatography–Mass Spectrometry (GC–MS) was used as a characterization tool in order to provide qualitative information on the composition of liquid and solid samples collected in gasification tests. Samples were dissolved in acetone for GC–MS analysis. A Fisons MD 800 quadrupole mass spectrometer interfaced to a Fisons GC 8060 gas chromatograph was used for GC–MS analysis. A Mega SE30 fused silica capillary column (25 m length, 0.32 mm internal diameter, cross-bonded, 0.25 μm film thickness) was employed for the chromatographic separation, with helium as carrier gas. The column temperature programme was as follows: 5 min isothermal at 40 °C, heating to 250 °C (6 °C/min), then 20 min isothermal. An injector temperature of 250 °C and splitless mode were used. Mass spectrometric detection was performed in full scan conditions (scan range, m/z 10–819) in electron impact ionization mode. The mass spectra obtained for each product were analyzed in order to obtain information about the molecular mass and the molecular structure. The structural identification of the products was achieved by comparison of their mass spectra with the best fits found in the NIST library or by analysis of the fragmentation patterns.

The water content of liquids and condensate sampled during gasification tests was determined by TG-FTIR analysis. TG-FTIR simultaneous measurements for the on-line analysis of volatile compounds formed during TG runs were carried out coupling a Netzsch STA 409/C thermoanalyzer with a Bruker Equinox 55 FTIR spectrometer. Calibration data for water were obtained with distilled water runs according to the vaporization-based pulse method extensively described elsewhere (Marsanich et al., 2002).

Gas composition was analyzed by a micro-GC Agilent 3000. This instrument allows analyzing hydrogen, light hydrocarbons and permanent gases in less than 240 s. The micro-GC was equipped with two independent channels based on an injector, a column and a thermal-conductivity detector (TCD). The first channel was based on a Molsieve 5A column, using argon as mobile phase and was suitable for the separation of hydrogen, oxygen, nitrogen, methane and carbon monoxide. The second channel was based on a PLOT U column using helium as mobile phase and suitable for the separation of carbon dioxide, ethane, ethylene and acetylene. The micro-GC was equipped with a pump for gas sampling and a membrane filter. The calibration of the instrument was performed with the Agilent Universal Gas Calibration Standard and the following gas mixtures provided by Rivoira: H_2 15.00%–N_2 85.00%, CH_4 2.997%–N_2 97.003%, C_2H_4 0.500%–N_2 99.500%, CO 0.995%–N_2 99.005%, CO 25.00%–N_2 75.00%, CO_2 1.50%–N_2 98.50%, and CO_2 19.98%–N_2 80.02%.

3. Results and discussion

3.1. Tests resume

Two sets of experiments were carried out for a total of five tests. Before starting the tests the reduction zone of the gasifier was fed with vegetal charcoal, in order to provide an initial char bed. Test 1 allowed substituting the initial charcoal bed with WSP char. Test 2 and 3 were performed with WSP as feedstock and bed. After Test 3 MIX was fed, so that after some hours of Test 4 the reduction zone was substituted with the char produced from MIX. Test 5 was entirely carried out with MIX as feedstock and char bed. The tests lasted from three to six hours. All tests were carried out with the aim to reach and keep constant the maximum syngas flow-rate. The pressure drop across the bed, the syngas flow-rate, the gas compositions and the clean-up temperatures were monitored throughout the tests.

3.2. Temperatures

TC-0 is the gasifier outlet temperature and thus can be considered as an indicator of the gasifier dynamic. The evolution of the

gasifier outlet temperature was similar in all tests; it took nearly two hours to reach a stable value which is close to 350 °C. The temperature at the cyclone outlet was 80–100 °C lower than the gasifier outlet, due to large thermal dispersion in the non insulated pipe. In the scrubber, gas was quenched to 20–40 °C due to contact with cold water. After the blower the syngas temperature increased due to the engine thermal dispersions, leading to a gas temperature of 30–50 °C.

The gasifier internal temperature was evaluated by moving a portable K thermocouple down through a nozzle and measuring the temperature in four positions as shown in Fig. 1c. The temperature at the nozzle outlet (position 0) was rather cool ranging from 334 to 431 °C. The temperature quickly increased as the thermocouple was moved down the throat. At 4 cm from nozzle outlet (position 1) the temperature ranged from 928 to 1086 °C (similar values have been reported by Martinez et al., 2012). As the thermocouple was moved deeper in the throat the temperature varied from 667 to 1109 °C and from 740 to 907 °C at 7 cm (position 2) and 10 cm (position 3) from the nozzle outlet, respectively. It seems that temperature reaches its maximum close to the nozzle outlet and subsequently decreases moving down the throat. This result is likely to be related to availability of oxygen in the throat. However, the position of the maximum temperature (and therefore of the burning front) can shift along the throat (as highlighted in Simone et al., 2011a and reported by Erlich and Fransson, 2011), probably due to continuous ignition of fresh biomass coming from the top or interaction with oxygen which is trapped in the hopper and released in the gasifier as the biomass is loaded (Balu and Chung, 2012).

3.3. Gasifier fluid dynamics

Significant differences in the gasifier behaviour were observed between Test 1 (gasifier reduction zone pre-loaded with vegetal charcoal) and other tests. Fig. 2 reports the evolutions of the pressure drop across the gasifier as well as the syngas flow-rate during Test 1 and Test 3. In the first part of Test 1 the syngas flow-rate was nearly constant at 90 $Nm^3\ h^{-1}$; subsequently it was gradually increased up to 130 $Nm^3\ h^{-1}$ by closing the by-pass valve. At 90 $Nm^3\ h^{-1}$ the pressure drop was stable below 100 mmH_2O and gradually increased as the syngas flow-rate was increased. After nearly three hours from the ignition, the gasifier pressure drop suddenly changed from 208 to 330 mmH_2O with the same syngas flow-rate. This indicates a change in the gasifier permeability which may be explained with the substitution of the pre-loaded charcoal with wood pellets char. In the early stage of Test 3 the syngas flow-rate was close to 100 $Nm^3\ h^{-1}$ but after half an hour a sudden increase in the gasifier pressure drop up to 400 mmH_2O occurred, with a consequent reduction in the syngas flow rate down to 70 $Nm^3\ h^{-1}$. During this stage it was not possible to control the syngas flow-rate by means of the by-pass until two hours from the ignition when the pressure drop dramatically decreased below 200 mmH_2O and it was possible to increase the syngas flow-rate up to 160 $Nm^3\ h^{-1}$. Table 2 reports average parameters for the five gasification tests. In Test 1 the average syngas flow rate was 112 $Nm^3\ h^{-1}$, the maximum flow rate was equal to 155 $Nm^3\ h^{-1}$, the average pressure drop was nearly 200 mmH_2O and the X ratio was 0.110, which fits very well with the optimal range. Tests with biomass pellets were characterized by lower flow-rates, higher pressure drop and lower X ratio. This indicates a lower bed permeability. Tests 2 and 3 show that with WSP it was possible to have some control of the bed (gas flow rate up to 160 $Nm^3\ h^{-1}$ could be reached), but the bed was characterized by higher pressure drops (nearly 240 mmH_2O) and the X ratio was close to the lower boundary (0.060). The situation was worse with MIX. In this case the pressure drop was higher (> 300 mmH_2O) indicating a reduction in the bed permeability, which did not allow to use the by-pass valve to control the gas flow-rate. This led to a de-rating of the gasifier output (maximum gas flow-rate 127 $Nm^3\ h^{-1}$) and operation out of the optimal gasification range ($X < 0.050$).

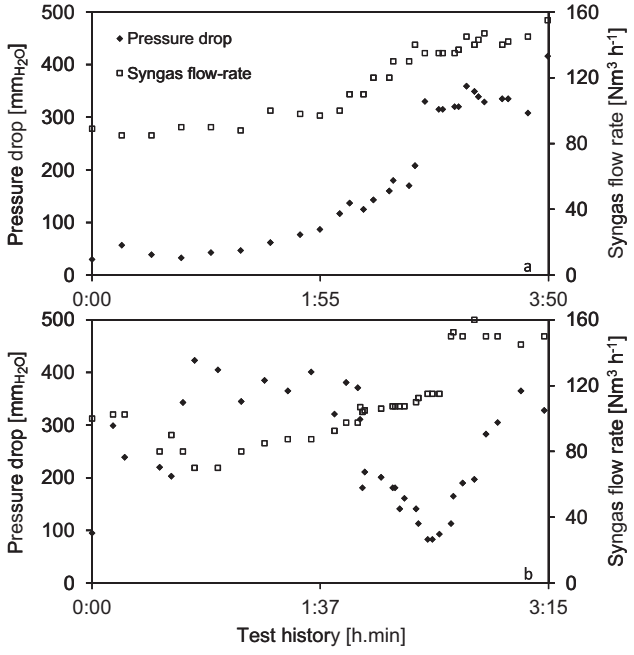

Fig. 2. Syngas flow rate and pressure drop evolutions during Test 1 (a) and Test 3 (b).

Noteworthy the pre-loaded vegetal charcoal is a solid material with high mechanical strength (compared to pellets) and mean size ranging from 30 to 50 mm, while biomass pellets are likely to break up due to mechanical and thermal stresses, thus generating dust into the gasifier. The formation of dust may explain the high resistance to flow, since the original size and shape of the biomass pellets are not very different from the charcoal. Sudden variations in the pressure drop may be explained with the substitution of dusty char with fresh material which retains (at least partially) the original morphology. Therefore the use of pelletized biomass in conventional downdraft gasifiers may lead to high and unstable pressure drops (for instance, preliminary tests with vine prunings exhibit average pressure drop close to 200 mmH_2O). High pressure drops reduce the syngas productivity and impose the use of high discharge frequencies leading to poor biomass conversions. In addition unstable pressure drops impose the brisk modulation of the discharge frequency which may destabilize the gasifier operation. These features are likely to be critical limitations for the use of biomass pellets in downdraft gasifiers. As reported by Dasappa et al. (2011), gasification systems based on fixed bed operate in optimal conditions when they are able to produce syngas without building up a resistance that could reduce the syngas productivity and the electrical load produced by the engine.

Table 2
Average syngas flow rate, pressure drop and X ratio achieved in the five tests (minimum and maximum values recorded in the test are reported in brackets).

Test	Pellet	Flow-rate ($Nm^3\ h^{-1}$)	ΔP_g (mmH_2O)	X (−)
1	WSP	112 (85–155)	203 (30–416)	0.110 (0.055–0.250)
2	WSP	94 (45–140)	234 (80–460)	0.062 (0.009–0.192)
3	WSP	105 (70–160)	245 (83–423)	0.062 (0.003–0.170)
4	MIX	101 (45–120)	308 (102–536)	0.039 (0.006–0.133)
5	MIX	84 (35–127)	350 (130–487)	0.030 (0.006–0.133)

Fig. 3 highlights the impact of the X ratio (see Eq. (4)) on the syngas flow rate during the gasification tests, compared with curves calculated according to a simplified mechanical energy balance over the plant at different openings of the by-pass valve (lines). Some of the experimental data are simply classified as partially open bypass, since it was not possible to evaluate the opening of the valve.

The simplified mechanical energy balance over the plant used to calculate the curves in Fig. 3 reads as:

$$\frac{W}{Q} = \Delta P_b + \Delta P_g + \Delta P_c + \Delta P_{by} \tag{5}$$

where W is the power provided by the blower, Q the syngas flow-rate, ΔP_b the pressure difference between the atmospheric and the blower outlet pressure, ΔP_g the pressure drop in the gasifier, ΔP_c the pressure drop in the clean-up system and ΔP_{by} the pressure drop in the by-pass.

The balance equation can be manipulated to obtain the following equation which expresses the syngas flow-rate (Q) as a function of X:

$$Q = \gamma_1 \cdot \sqrt{\frac{W - \Delta P_b}{k_c + k_b \cdot \left(\frac{1-\alpha}{\alpha}\right)^2 + \gamma_2 \cdot \left(\frac{1-X}{X}\right)}} \tag{6}$$

where γ_1 and γ_2 are constants which depend on the gasifier geometry, gas density and compositions, α represents the by-pass valve opening (1 corresponds to closed by-pass, 0.4 corresponds to open by-pass), k_c and k_b are empirical constants that multiplied by the square velocity allow to calculate the pressure drop in the clean-up system and the by-pass.

As can be seen in Fig. 3, when the X ratio is lower than 0.05 the by-pass valve has almost no effect on the pressure drop and the syngas flow-rate, since the gas flow is almost completely controlled by the very low permeability of the gasifier bed. As X increases, it is possible to modulate the syngas flow rate. After 0.2 the curves are close to asymptotic values, therefore the gas flow in the plant is controlled by other resistances. This situation may indicate the formation of preferential channels or an excessive permeability of the bed which may switch to combustion mode.

3.4. Gas composition

Fig. 4 reports the evolution of the syngas composition during three tests and Table 3 the average composition obtained from each test. After nearly 15 min from the ignition the nitrogen content reached a steady value close to the average reported in Table 3. In this initial stage the carbon monoxide content was higher than the steady state value, while the hydrogen and carbon dioxide contents were lower. It took from 45 min to 1 h to reach a stable syngas composition. During this time the hydrogen and carbon dioxide contents increased, while the carbon monoxide decreased (as discussed in Simone et al., 2011a). After 1 h the syngas

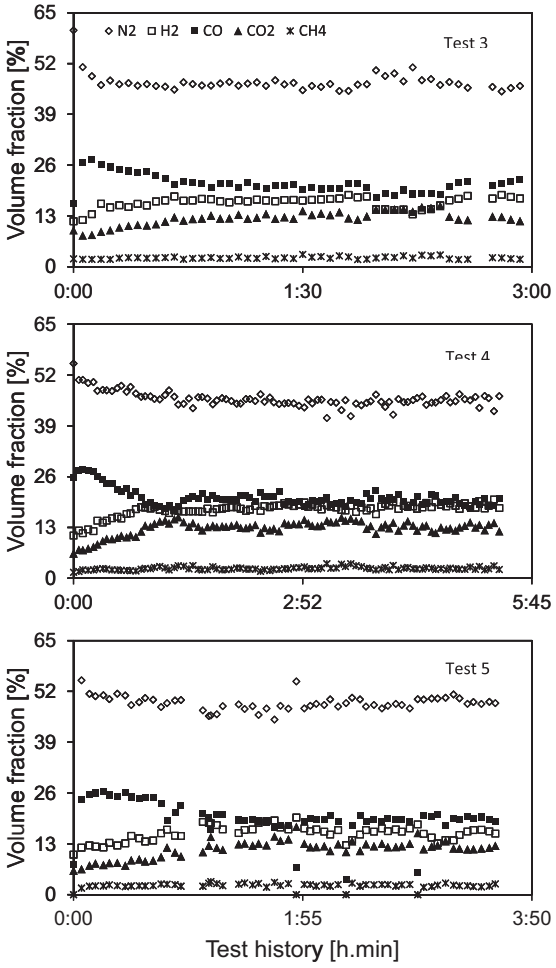

Fig. 4. Gas composition evolution during Tests 3, 4 and 5.

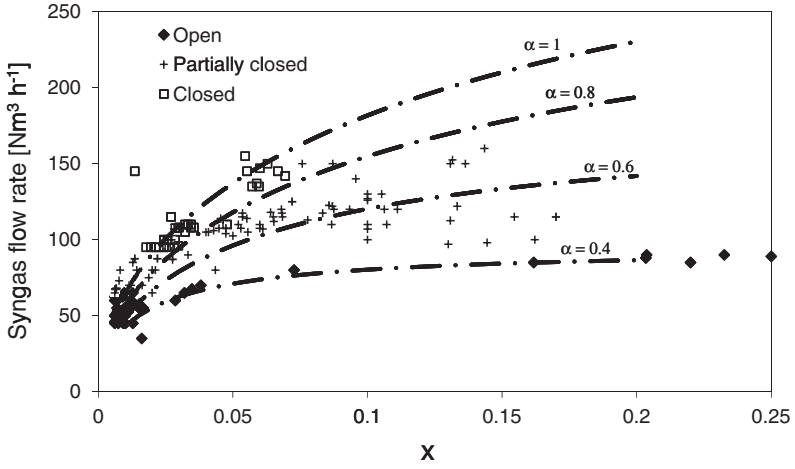

Fig. 3. Syngas flow-rate as a function of the X ratio. Dots: experimental data; Lines: curves calculated according to the pressure curve of the system with different openings of the by-pass valve.

Table 3
Gas compositions obtained from gasification tests of pelletized biomass and calculated according to an equilibrium model of the gasifier.

Experimental tests	Pellet	CO (%)	H_2 (%)	CO_2 (%)	N_2 (%)	CH_4 (%)	C_2H_4 (%)	LHV (MJ Nm^{-3})
1	WSP	21.3	17.5	13.3	44.2	3.1	0.5	6.0
2	WSP	21.6	17.6	12.0	46.0	2.3	0.4	5.7
3	WSP	21.3	16.3	12.4	47.2	2.3	0.4	5.5
4	MIX	20.6	17.6	12.8	45.9	2.5	0.5	5.7
5	MIX	19.7	15.8	11.6	49.5	2.3	0.8	5.6
Equilibrium calculation								
T = 853 K	WSP	10.0	14.8	20.7	50.2	4.3	–	–
T = 893 K	WSP	15.5	17.3	16.8	46.8	3.6	–	–
T = 933 K	WSP	22.0	18.5	13.2	43.4	2.9	–	–

composition was rather stable. The syngas was mainly composed of hydrogen, carbon monoxide, carbon dioxide, nitrogen, methane and ethylene; ethane and acetylene were detected as well in lower concentrations (<0.1%). The average syngas composition was quite similar for the five tests. Tests 1–4 exhibited very close compositions, irrespectively of the feedstock and the char bed. The syngas compositions are similar to those reported in the literature (for instance Martinez et al. (2012)). Test 5 exhibited carbon monoxide, carbon dioxide and hydrogen contents lower than the other tests. Fig. 4 shows some large fluctuations in the gas composition of Tests 5, with high nitrogen and low carbon monoxide contents, which affect the average composition. However, the lower hydrogen, carbon dioxide as well as carbon monoxide contents may indicate a lower conversion of the fuel into syngas which could be either due to a bad fluid-dynamic in the gasifier (as confirmed by the large fluctuations) or to the higher ash content of MIX compared to WSP.

The syngas LHV of Test 1 was higher than the other tests. This may be related to the vegetal charcoal used to pre-load the gasifier reduction zone which allows for better control of the gasifier operation. The syngas LHV was stable in the other tests ranging from 5.52 to 5.75 MJ Nm^{-3}. Test 5 exhibited a LHV close to Test 2, 3, 4 despite the lower hydrogen and carbon monoxide content; this is due to the higher ethylene content, which on the other hand might indicate higher tar generation.

Table 3 reports also compositions for wood pellets obtained from simple calculations assuming stoichiometric combustion in the oxidation zone and equilibrium conditions (at different temperatures) in the reduction zone where the following reactions are considered:

$$C + CO_2 \rightleftharpoons 2\ CO$$
$$C + H_2O \rightleftharpoons H_2 + CO$$
$$C + 2\ H_2 \rightleftharpoons CH_4$$
$$CO + H_2O \rightleftharpoons CO_2 + H_2$$

The temperature profile of the reduction zone ranges between 800–700 °C and 500–400 °C, therefore the mean temperature is varied between 580 and 660 °C. Assuming a mean temperature of 580 °C leads to relatively high nitrogen content, which indicates a poor conversion of the solid material, high carbon dioxide and low carbon monoxide, indicating that the equilibrium of the Boudouard reaction is shifted towards carbon dioxide. Increasing the mean temperature of the reduction zone leads to more satisfactory values, reducing the methane, carbon dioxide and nitrogen contents and increasing the carbon monoxide and hydrogen contents. The compositions calculated at 933 K (660 °C) are comparable to the experimental values (in particular Test 1). However lower temperatures of the reduction zone are required to match the carbon monoxide, hydrogen and nitrogen contents, conversely higher temperatures are required to fit better carbon dioxide and methane (Tests 2 and 3). Therefore it seems that equilibrium calculations can provide a good indication of the final syngas composition, nevertheless stoichiometric oxidation and the equilibrium of the reduction zone do not represent completely the behaviour of the gasifier, highlighting the influence of kinetics and transport phenomena on the process. However, other models based on equilibrium approach but including the heat balance (Balu and Chung, 2012) and modifications of the equilibrium expression of the carbon gasification reaction with hydrogen (Barman et al., 2012; Jarungthammachote and Dutta, 2007) were found to provide more accurate results. To this purpose a more detailed modelling approach will be the object of a forthcoming paper.

3.5. Liquids sampling and analysis

The condensate sampling was carried out in Tests 3, 4 and 5. On the average the condensable fraction of the gas was found to be 35 g Nm^{-3} of gas. The TG-FTIR analysis of the condensate showed water content of 34 g Nm^{-3} of gas. The remaining fraction can be attributed to condensed organic compounds (approximately 1 g Nm^{-3} of gas). The condensate was subjected to GC–MS analysis in order to identify the organic compounds present. Only few species could be detected: acetic acid, propanoic acid, phenol, cresol. Since these compounds are water soluble, they can contaminate the water used for gas scrubbing.

3.6. Solid sampling and analysis

3.6.1. Gasification residues

The gasifier residues discharged from the gasifier bottom in the collection tank were sampled during Tests 1, 3, 5 (named C1, C3 and C5). C1 contains relatively big particles (average size 1 cm), while the particles in C3 and C5 are in the range 1–2 mm.

The final size of the gasification residues has a great impact on the process performance. The screw conveyor of the collection tank was able to handle only C1 residues but not the finer C3–C5 residues. As a consequence it was not possible to collect the charcoal and the water of the collection tank was highly polluted with suspended solids. Table 1 reports the composition of the three samples. The three samples exhibit high carbon contents (>80%) and relatively high LHV (nearly 25 MJ/kg). These residues can therefore be used for thermal applications. An attempt was made to estimate the conversion of the organic material according to the ash content of original biomass (WSP and MIX) and charry residues (C3 and C5). The conversion values result 75.7% for WSP and 36.8% for MIX. These values are not realistic. In particular the conversion of MIX is too low and scarcely fits with the composition of C5 which is almost completely devolatilized. Therefore the conversion of the organic material in the gasification process cannot be estimated according to the ash content in the residues.

3.6.2. Gasifier bed

After Test 5 an attempt was made to sample the gasifier bed from the air nozzles (named BED). Table 1 reports the proximate and ultimate composition of BED. This sample contains nearly

55% of volatile matter; therefore it seems that the devolatilization process is still occurring at the nozzle outlet. This result might be in agreement with the theory of flaming pyrolysis proposed by Reed and Markson (1985). In BED the original WSP particles can be easily recognized, these particles are similar in size and shape to the original ones. On the other hand SMP particles cannot be recognized (even if their presence is verified by the relevant nitrogen content) thus their mechanical resistance is likely to be lower than WSP.

3.6.3. Particulates

After Test 5 two particulates samples were collected from the plant. The samples are:

- PO, collected at the gasifier outlet in the proximity of TC0 by removing the pipe in this position.
- PC, collected at the bottom of the tank positioned under the cyclone for particulates removal.

Table 1 reports the proximate and ultimate analysis of the two samples. PC is a charry material but not completely devolatilized. The composition of PO is not easy to be interpreted; this residue is likely to be a mixture of different deposits (organic particulates and tar). The chromatograms obtained from the GC–MS analysis of the acetone extracts of PO and PC, indicate the presence of complex mixtures of organic compounds. The chromatogram of PA is shifted toward higher retention time than PC. This may indicate the presence of heavier compounds in PO than in PC. Not all the detected species could be identified; however, an identification of the chemical structure was possible for many chromatographic peaks (Table 4). Except for phenols (the lightest compounds) and benzofurans, all the extracted components in PO are polycyclic aromatic hydrocarbons (PAH) ranging from naphthalene to coronene. These compounds are likely to condense immediately at the gasifier outlet. The composition of the PC extract is somewhat similar to that of PO, containing many PAH such as naphthalene and anthracene. However, the presence of light compounds such as acetic and propanoic acid indicates that this extract is slightly shifted toward lighter compounds. Given these results and the lack of heavy tar in the sampled condensate it can be stated that heavy tar condenses in the plant before reaching the scrubber and the tar sampling point. It is likely that in the early stage of process heavy tar condenses immediately at the gasifier outlet due to the low temperature. As the temperature increases the condensation point is shifted toward the cyclone where the temperature is below 250 °C. Here almost all the fractions condense and a broad range of compounds can be identified in PC. Therefore the tar content at the sampling point is much lower than at the gasifier outlet and its composition is qualitatively shifted towards light compounds. On the basis of this result the composition of PO can be explained as a mixture of charry particles with a high conversion (which explains the high ash content) and some condensed PAH (which explains the volatile matter content in this charry material).

Table 4
Organic compounds identified by GC–MS analysis in the extracts of particulate samples PO and PC.

Compound	Chemical formula	Molecular weight	PO	PC
Acetic acid	$C_2H_4O_2$	60		x
Propanoic acid	$C_3H_6O_2$	74		x
Butyrolactone	$C_4H_6O_2$	86		x
Phenol	C_6H_6O	94	x	x
Methylcyclopentenone	C_6H_8O	96		x
Methylphenol	C_7H_8O	108	x	x
Indene	C_9H_8	116	x	x
Dimethylphenol	$C_8H_{10}O$	122		x
Naphthalene	$C_{10}H_8$	128	x	x
Methylindene	$C_{10}H_{10}$	130		x
Isopropylphenol	$C_9H_{12}O$	136		x
Methoxycresol	$C_8H_{10}O_2$	138		x
Methylnaphthalene	$C_{11}H_{10}$	142	x	x
Isopropylmethylphenol	$C_{10}H_{14}O$	150		x
Acenaphthylene	$C_{12}H_8$	152	x	
Biphenyl	$C_{12}H_{10}$	154	x	x
Acenaphthene	$C_{12}H_{10}$	154	x	x
Dimethylnaphthalene	$C_{12}H_{12}$	156	x	x
Ethylnaphthalene	$C_{12}H_{12}$	156	x	
Fluorene	$C_{13}H_{10}$	166	x	x
Phenalene	$C_{13}H_{10}$	166		x
Dibenzofuran	$C_{12}H_8O$	168	x	x
Methylbiphenyl	$C_{13}H_{12}$	168	x	x
Isopropylnaphthalene	$C_{13}H_{14}$	170	x	
Trimethylnaphthalene	$C_{13}H_{14}$	170		x
Anthracene/phenanthrene	$C_{14}H_{10}$	178	x	x
Methylfluorene	$C_{14}H_{18}$	180	x	x
Methyldibenzofuran	$C_{13}H_{10}O$	182		x
Methylanthracene	$C_{15}H_{12}$	192	x	
Methylphenanthrene	$C_{15}H_{12}$	192	x	x
Fluoranthene	$C_{16}H_{10}$	202	x	x
Pyrene	$C_{16}H_{10}$	202	x	x
Phenylnaphthalene	$C_{16}H_{12}$	204	x	x
Ethylphenanthrene	$C_{16}H_{14}$	206	x	
Dimethylphenanthrene	$C_{16}H_{14}$	206	x	x
Methylpyrene	$C_{17}H_{12}$	216	x	x
Benzo[*c*]fluorene	$C_{17}H_{12}$	216	x	x
Benzonaphthofuran	$C_{16}H_{10}O$	218	x	x
Trimethylphenanthrene	$C_{17}H_{16}$	220	x	x
Benzo[ghi]fluoranthene	$C_{18}H_{10}$	226	x	x
Benzo[*a*]anthracene	$C_{18}H_{12}$	228	x	x
Benzo[*c*]phenanthrene	$C_{18}H_{12}$	228	x	x
5,6-Dihydrochrysene	$C_{18}H_{14}$	230	x	
Tetramethylphenanthrene	$C_{18}H_{18}$	234	x	x
Methylchrysene	$C_{19}H_{14}$	242	x	
Benzo[*b*]fluoranthene, Benzo[*j*]fluoranthene, Benzo[*k*]fluoranthene, Benzo[*e*]pyrene, perylene	$C_{20}H_{12}$	252	x	x
Benzo[ghi]perylene, Indeno[1,2,3-cd]pyrene	$C_{22}H_{12}$	276	x	x
Dibenzo[*a,j*]anthracene	$C_{22}H_{14}$	278	x	
Coronene	$C_{24}H_{12}$	300	x	x
Dibenzopyrene	$C_{24}H_{14}$	302	x	x

3.7. Energy and material balances

The gasification performance can be evaluated for the two feedstock according to the cold gas efficiency and the specific gas production. To calculate these indicators it is necessary to characterize the material, elemental and energy balance of the plant. The balances performed in this work rely on some assumptions:

- particulates and tar productions are assumed to be negligible compared to the gas output;
- the biomass loading rate is calculated as the total mass of feedstock charged over the time elapsed from the gasifier ignition (consequently it is an average loading rate);
- the syngas volumetric flow-rate is estimated by averaging the rotameter readings on the total elapsed time;
- the incoming air flow-rate is calculated by assuming that all the nitrogen in the syngas is equal to nitrogen entering the system with air (i.e. the nitrogen in the biomass and charry residue is neglected).

On the basis of the material balance, the elemental balance can be drawn from the biomass and charry residue ultimate analysis and syngas compositions.

The balances are calculated for two groups of tests. The first group is related to WSP gasification (Tests 1, 2 and 3) and it is named B1, while the second group (named B2) including Tests 4 and 5 is related to MIX.

As mentioned in Section 3.6.1 the composition of the gasification residues cannot be considered completely reliable. On the other hand, formulating a hypothesis for the composition of the charry residue would affect too much the results, therefore an optimization approach was chosen: the gasification residue is assumed to be composed of carbon and ash, and the relative proportion of the two fractions is varied in order to minimize the closure of the material, elemental and energy balance. The results of the calculations are reported in Table 5. Good closures of the mass and energy balance are achieved both for B1 and B2. On the other hand it is rather difficult to achieve good closures of the elemental balances, in particular for carbon. However, except for carbon, deviations are within 10%. Table 5 reports the results of the mass balance. These data are related to average conditions during the group of tests. The two tests were similar. However the biomass loading rate was slightly higher in B1 than B2, generating higher syngas flow-rate and requiring a higher air flow-rate. It is worthy to note that pelletized biomass led to a low throughput of the gasifier since the average gas flow rates ranges from 97.5 to 106.3 N m^3 h^{-1}. Preliminary tests with looser feedstock (vine prunings) allowed a stable production of 120 N m^3 h^{-1}. However the gasification of pelletized biomass produced a good quality syngas. On the basis of the biomass load and air flow-rate it is possible to evaluate the equivalence ratio (ER). The ER is very similar for the two groups (0.30 vs. 0.29) despite the different biomass loading rate and syngas production. Noteworthy this is an average data and as matter of facts the ER is variable throughout the test according to the biomass loading rate and the air flow-rate fluctuations due to variation of the bed permeability. The data achieved from the mass and energy balance allows calculating the specific gas production (PS – N m^3 syngas per kg wet biomass) and the cold gas efficiency (CGE – energy output associated to the cold syngas/energy input associated to the biomass). The results are reported in Table 5. B2 exhibits slightly higher values of specific gas production (2.4 vs. 2.2) and CGE (70% vs. 67.7%), but if the error associated to the balance calculation is taken into account the performance of the two sets of tests can be considered almost equal. A straight comparison of the gasification performance of the two feedstock is not possible since it was not possible to operate the tests in the same operating conditions (biomass loading rate and air flow-rate). It is worthy to note that these values are comparable to those reported in the literature for biomass gasification with air in downdraft gasifiers, the specific production range is 1.8–2.5 (Dogru et al., 2002; Erlich and Fransson, 2011; Martinez et al., 2012; Sheth and Babu, 2010) and the cold gas efficiency range is 50–76.7 (Erlich and Fransson, 2011; Martinez et al., 2012; Pathak et al., 2008; Zainal et al., 2002).

Table 5
Closures of the material, elemental and energy balance, mass balance results and performance indicators for the two groups of tests.

	Units	B1	B2
Balance closure			
Mass	%	99.0	98.5
Carbon	%	88.3	89.5
Oxygen	%	105.1	99.5
Hydrogen	%	109.8	102.5
Energy	%	104.3	102.0
Ash contents			
Sampled residue	%	8.65	7.90
Calculated residue	%	16	35
Results			
Biomass load	kg h^{-1}	54.2	44.7
Air flow-rate	Nm^3 h^{-1}	63.1	60.4
Syngas flow-rate	Nm^3 h^{-1}	106.3	97.5
Water production	kg h^{-1}	9.57	8.77
Residue production	kg h^{-1}	6.30	5.78
ER	–	0.30	0.29
Performance			
PS	Nm^3 kg^{-1}	2.2	2.4
CGE	%	67.7	70.0

4. Conclusions

The gasification facility equipped with on-line and off-line measurement devices has been a powerful tool for studying the gasification behaviour and process characteristics of different biomass. The results of five gasification tests prove that pelletized biomass is not an ideal feedstock for downdraft gasifiers, due to high pressure drops, difficult gasifier control and fragmentation of the gasification residues. However, the gas composition and global performance indicators were quite satisfactory, therefore pelletized biomass may be used as complementary feedstock to increase the energy content per volume and reduce the moisture effects.

Acknowledgements

This work was carried out with the facilities of the Centro di Ricerca Interuniversitario Biomasse da Energia (CRIBE) and benefited of the financial support provided by the Fondazione Cassa di Risparmio di Pisa.

References

Balu, E., Chung, J.N., 2012. System characteristics and performance evaluation of a trailer-scale downdraft gasifier with different feedstock. Bioresour. Technol. 108, 264–273.
Barman, N.S., Ghosh, S., De, S., 2012. Gasification of biomass in a fixed bed downdraft gasifier – A realistic model including tar. Bioresour. Technol. 107, 505–511.
Barontini, F., Simone, M., Ragaglini, G., Mancini, A., D'Alvano, S., Triana, F., Nicolella, C., 2011. From Crop to Biofuels: a Case study of sunflower crude oil production in Tuscany. Proc. 19th Eur. Biomass Conf. Exhib. 2062–2069.
Dasappa, S., Subbukrishna, D.N., Suresh, K.C., Paul, P.J., Prabhu, G.S., 2011. Operational experience on a grid connected 100 kWe biomass gasification power plant in Karnataka. Indian Energ. Sust. Develop. 15, 231–239.
Dogru, M., Howarth, C.R., Akay, G., Keskinler, B., Malik, A.A., 2002. Gasification of hazelnut shells in a downdraft gasifier. Energy 27, 415–427.
Erlich, C., Fransson, T.H., 2011. Downdraft gasification of pellets made of wood, palm-oil residues respective bagasse: experimental study. Appl. Energy 88, 899–908.
Garcia-Bacaicoa, P., Mastral, J.F., Ceamanos, J., Berrueco, C., Serrano, S., 2008. Gasification of biomass/high density polyethylene mixtures in a downdraft gasifier. Bioresour. Technol. 99, 5485–5491.
Hassler, P., Buehler, R., Nussbaumer, T., 1997. Evaluation of Gas Cleaning Technologies for Small Scale Biomass Gasifiers. Swiss Federal Office of Energy, Berne.
Jarungthammachote, S., Dutta, A., 2007. Thermodynamic equilibrium model and second law analysis of a downdraft waste gasifier. Energy 32, 1660–1669.
Marsanich, K., Barontini, F., Cozzani, V., Petarca, L., 2002. Advanced pulse calibration techniques for the quantitative analysis of TG-FTIR data. Thermochim. Acta 390, 153–168.
Martinez, J.D., Mahkamov, K., Andrade, R.V., Silva Lora, E.E., 2012. Syngas production in downdraft biomass gasifiers and its application using internal combustion engines. Renewable Energy 38, 1–9.
Midilli, A., Dogru, M., Howarth, C.R., Ayhan, T., 2001. Hydrogen production from hazelnut shell by applying air-blown downdraft gasification technique. Int. J. Hydrogen Energy 26, 29–37.
Pathak, B.S., Patel, S.R., Bhave, A.G., Bhoi, P.R., Sharma, A.M., Shah, N.P., 2008. Performance evaluation of an agricultural residue-based modular throat-type down-draft gasifier for thermal application. Biomass Bioenergy 32, 72–77.
Reed, T.B., Markson, M., 1985. Biomass gasification reaction velocities. In: Overend, R.P., Milne, T.A., Mudge, L.K. (Eds.), Fundamentals of Thermochemical Biomass Conversion. Elsevier, Amsterdam, pp. 951–966.
Sharan, H., Buhelr, R., Giordano, P., Hasler, P., Salzmann, R., Dasappa, S., Sridhar, B., Girish, B., 1997. Adaptation of the IISC-Dasag Gasifier for Application in Switzerland. Swiss Federal Office of Energy, Berne.
Sharma, A.K., 2011. Experimental investigations on a 20 kWe, solid biomass gasification system. Biomass Bioenergy 35, 421–428.
Sheth, P.N., Babu, B.V., 2010. Production of hydrogen energy through biomass (waste wood) gasification. Int. J. Hydrogen Energy 35, 10803–10810.
Simone, M., Guerrazzi, E., Biagini, E., Nicolella, C., Tognotti, L., 2009. Technological barriers of biomass gasification. Int. J. Heat Technol. 27, 127–132.

Simone, M., Barontini, F., Nicolella, C., Tognotti, L., 2011a. Experimental characterization of the performance of a biomass downdraft gasifier. Fifth European Combustion Meeting.

Simone, M., Barontini, F., Ierna A., Nicolella, C., Tognotti, L., 2011b. Biomass tar: assessment of a sampling device and characterization methodology. In: Proceedings of 19th European Biomass Conference on Exhibition, pp. 1432–1439.

Wander, P.R., Altafini, C.R., Barreto, R.M., 2004. Assessment of a small sawdust gasification unit. Biomass Bioenergy 27, 467–476.

Zainal, Z.A., Rifau, A., Quadir, G.A., Seetharamu, K.N., 2002. Experimental investigation of a downdraft biomass gasifier. Biomass Bioenergy 23, 283–289.